Risks to carbon storage from land-use change revealed by peat thickness maps of Peru

Adam Hastie[1], Eurídice N. Honorio Coronado[2,3], José Reyna[3], Edward T. A. Mitchard[1], Christine M. Åkesson[2], Timothy R. Baker[4], Lydia E. S. Cole[2], César. J. Córdova Oroche[3], Greta Dargie[4], Nállarett Dávila[3], Elsa Carla De Grandi[1], Jhon Del Águila[3], Dennis Del Castillo Torres[3], Ricardo de la Cruz Paiva[5], Frederick C. Draper[4,6], Gerardo Flores[3], Julio Grández[3], Kristell Hergoualc'h[7], J. Ethan Householder[8], John P. Janovec[9], Outi Lähteenoja[10], David Reyna[3], Pedro Rodríguez-Veiga[11,12], Katherine H. Roucoux[2], Mathias Tobler[13], Charlotte E. Wheeler[1,7], Mathew Williams[1,14], Ian T. Lawson[2].

Affiliations

1 School of GeoSciences, University of Edinburgh, Edinburgh, United Kingdom
2 School of Geography and Sustainable Development, University of St Andrews, St Andrews, United Kingdom
3 Instituto de Investigaciones de la Amazonía Peruana (IIAP), Av. Abelardo Quiñonez km 2.5, Iquitos, Perú
4 School of Geography, University of Leeds, Leeds, United Kingdom
5 Servicio Nacional Forestal y de Fauna Silvestre, Avenida Javier Prado Oeste, Magdalena del Mar, Lima, Perú
6 Center for Global Discovery and Conservation Science, Arizona State University, AZ, United States of America
7 Center for International Forestry Research (CIFOR), Jl. CIFOR, Situ Gede, Bogor, 16115, Indonesia
8 Wetland Ecology, Institute for Geography and Geoecology, Karlsruhe Institute for Technology, Karlsruhe, Germany
9 Sam Houston State University Natural History Museum, Sam Houston State University, Huntsville, TX, USA
10 Helsinki, Finland
11 Centre for Landscape and Climate Research (CLCR), School of Geography, Geology and Environment, University of Leicester, University Road, Leicester LE1 7RH, UK
12 National Centre for Earth Observation, University of Leicester, Space Park Leicester, Corporation Road, Leicester LE4 5SP, UK
13 San Diego Zoo Global, Institute for Conservation Research, 15600 San Pasqual Valley Road, Escondido, CA, USA
14 NCEO, University of Edinburgh, UK

Abstract

Tropical peatlands are among the most carbon dense ecosystems but land-use change has led to the loss of large peatland areas, associated with substantial greenhouse gas emissions. In order to design effective conservation and restoration policies, maps of the location and carbon storage of tropical peatlands are vital. This is especially so in countries such as Peru where the distribution of its large, hydrologically intact peatlands is poorly known. Here, field and remote sensing data support model development of peatland extent and thickness for lowland Peruvian Amazonia. We estimate a peatland area of 62,714 (5th and 95th confidence interval percentiles 58,325–67,102 respectively) km^2 and carbon stock of 5.4 (2.6–10.6) Pg C, a value approaching the entire above-ground carbon stock of Peru but contained within just 5% of its land area. Combining the map of peatland extent with national land-cover data we reveal small but growing areas of deforestation and associated CO_2 emissions from peat decomposition, due to conversion to mining, urban areas, and

agriculture. The emissions from peatland areas classified as forest in 2000 represent 1–4% of Peruvian CO_2 forest emissions between 2000 and 2016. We suggest that bespoke monitoring, protection and sustainable management of tropical peatlands are required to avoid further degradation and CO_2 emissions

Main text

While tropical peatlands are known to be among the most carbon-dense ecosystems in the tropics[1,2], their absolute contribution to the global carbon cycle remains highly uncertain, with recent estimates placing their total below-ground carbon storage between 105 (70–130) and 215 (152–288) Pg C[3,4]. They face various threats including land-use and climate change[4,5]. Deforestation and/or drainage of peatlands inhibit the accumulation of organic matter and promotes rapid decomposition of peat, releasing large quantities of the greenhouse gasses (GHG) CO_2 and N_2O to the atmosphere[6,7,8,9,10]. Moreover, drained peatlands are prone to fires which lead to large pulses of emissions[11]. The experience of Indonesia provides a cautionary tale: in 1997 alone, it was estimated that between 0.81 and 2.57 Pg C were released as a result of peat and vegetation fires, which at the time equated to 13–40% of global fossil fuel emissions[12]. Indeed, the peatlands of Southeast Asia have already been severely damaged with almost 80% cleared and drained[13]. In contrast, the largest known peatland areas in tropical Africa and South America are thought to remain largely intact[14,15].

As such, commitments to avoid further deforestation and degradation by 1) promoting conservation and sustainable management of intact peatlands and 2) restoring degraded peatlands, are essential to reducing CO_2 emissions and avoiding global warming of 1.5°C or more[16,17]. A funding mechanism for this is potentially offered by UNFCCC initiatives, including REDD+ and wider National Determined Contributions[18] to the Paris Agreement,

65 but a necessary first step towards conservation and restoration is reliable mapping of the
66 spatial distribution of peatlands and their carbon stocks, at scales relevant to the
67 development of national policies.

68 Peru has substantial known regions of hydrologically intact peatland. Previous research
69 identified a large area in the Pastaza-Marañón Foreland Basin in northern Peru (PMFB, Fig.
70 S1), estimating its carbon stock to be 3.14 (0.44–8.15) Pg C including above- and below-
71 ground carbon[2], and a smaller area in the Madre de Dios (MDD) region of southern Peru
72 holding an estimated 0.03 Pg C[19]). However, published wetland maps[20,21] and visual
73 examination of remote sensing imagery suggest that there are likely other significant
74 peatlands in Peru whose carbon stocks remain unquantified. Even in the best-known region,
75 the PMFB, previous mapping was based on relatively small numbers of peat thickness
76 measurements and did not attempt to model and map the spatial variation in peat
77 thickness[2,22], one of the greatest sources of uncertainty in the below-ground carbon stock[2].
78 Rather, the total below-ground carbon stock for the PMFB was estimated by determining
79 the area of different peat-forming vegetation classes (i.e. peatland pole forest, palm swamp
80 and open peatland) and multiplying those areas by a mean below-ground carbon stock for
81 each vegetation class. This approach makes several simplifying assumptions[23]: that these
82 three vegetation classes are always underlain by peat, that peat thickness varies more
83 between than within classes, and that other landcover classes (including some wetland
84 ecosystems such as seasonally flooded forest) never overlie peat[2,22]. In fact, field
85 observations indicate that these assumptions are no longer valid; in particular, peat
86 thickness varies substantially in space, including within single vegetation classes[3,23]. Data-
87 driven maps that more accurately capture the spatial variation in peat thickness and carbon

88 storage, and that cover not just selected study areas but the whole of Peruvian Amazonia,
89 are required to support national and regional peatland conservation planning.

90 While Peruvian peatlands are believed to remain largely intact, thus far there has been no
91 quantitative assessment of GHG emissions resulting from landcover change. Moreover, they
92 face varied and increasing threats including agriculture expansion, illegal mining, oil
93 exploration, infrastructure development, and the selective felling of the female *Mauritia*
94 *flexuosa* palm for commercial purposes[15,23,24,25,26]. In recognition of these threats, legislation
95 has recently been enacted which, for the first time, mandates the explicit protection of
96 peatlands in Peru for climate-change mitigation[27]. Enforcing this legislation effectively will
97 depend on robust mapping of peatland distribution, and on knowledge of the scale and
98 distribution of recent peatland disturbance, none of which is presently available.

99 Here we present extensive new field observations (Fig. 1) to test whether previous evidence
100 of a relationship between distance to peatland edge and peat thickness found in other
101 tropical peatlands[3], also applies in Peru. These data are used along with remote sensing
102 imagery to develop the first data-driven models of peatland extent and peat thickness
103 distribution across the whole of lowland Peruvian Amazonia (LPA). We quantify the spatial
104 variation and total peat carbon stock of these peatlands, and associated uncertainties.
105 Finally, we use these models, along with national data on land-cover change, to map
106 peatland disturbance and estimate the associated CO_2 emissions for the period 2000–2016.

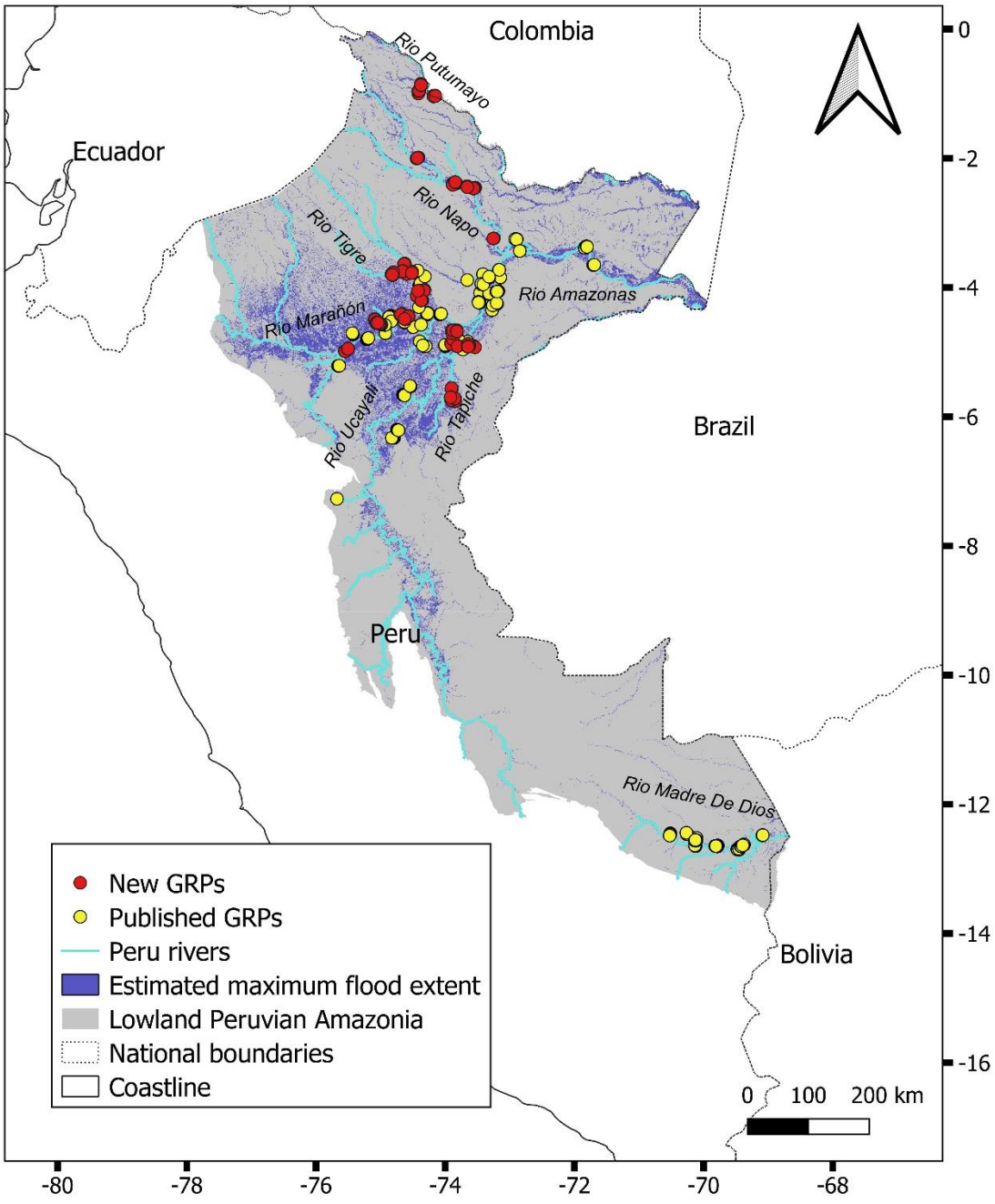

Figure 1: Distribution of the 1,128 ground reference points (GRPs) sampled for peat thickness and vegetation type data used in this study. The points include GRPs collected from 2019-2021 as part of this study (red, n = 445) as well as published GRPs from[2,19,22,28] (yellow). Estimated maximum flood extent is derived from the wetlands map of ref. [20]. Rivers of Strahler order ≥ 6 are shown.

Peat thickness distribution reveals a large carbon store

We estimate a total peatland extent of 62,714 (58,325–67,102) km^2 (Fig. S2), a mean peat thickness of 203 (179–224) cm (Fig. 2, Fig. S3) and a total below-ground carbon stock of 5.38 (2.55–10.58) Pg C (Fig. S4) across the LPA. In addition to the well-known peatlands of the PMFB and MDD basin, we identify substantial areas of peatland in the Ucayali (11,110 km^2; 2,258 km in Tapiche sub-basin), Napo (3,670 km^2) and Putumayo (2,319 km^2) basins (Fig. 2, Fig. S1, Table S1). Palm swamp is the most extensive peat-forming ecosystem (46,423 km^2) and therefore contains the greatest stock (3.83 Pg C), despite pole forest and open peatland having higher peat carbon densities (1,054 Mg C ha^{-1} and 1,061 Mg C ha^{-1} respectively, Table S2). We estimate that 2% of seasonally flooded forest overlies peat, equating to an area of 1,951 km^2 and a peat C stock of 0.11 Pg C (Table S2).

The distribution of peat thickness across the LPA is highly variable, with the greatest mean peat thickness predicted in the Tigre (232 cm), Marañón (230 cm), Tapiche (234 cm), and Napo basins (223 cm) (Fig. 2, Table S1). Our models of peatland area and peat thickness distribution performed well against observations (Table S3, Fig. S5), giving confidence in our results. We ran two separate peat thickness models: one for the MDD basin and another for all the rest of the study area (which contains 97% of total peatland area). The model which excluded the MDD basin performed better ($p < 0.0001$; $R^2 = 0.66$, RMSE = 66%, Fig. S5a) than the MDD model ($p < 0.0001$; $R^2 = 0.38$, RMSE = 70%, Fig. S5b). We found a significant linear relationship between peat thickness and distance to peatland edge ($p < 0.0001$, $R^2 = 0.13$, Fig. S6a). This relationship was more significant when the data from the MDD basin were excluded (giving $R^2 = 0.39$, $p < 0.0001$, Fig. S6b) and there was no significant

relationship between peat thickness and distance to peatland edge within the MDD data ($p > 0.1$, $R^2 = 0.005$, Fig. S6c).

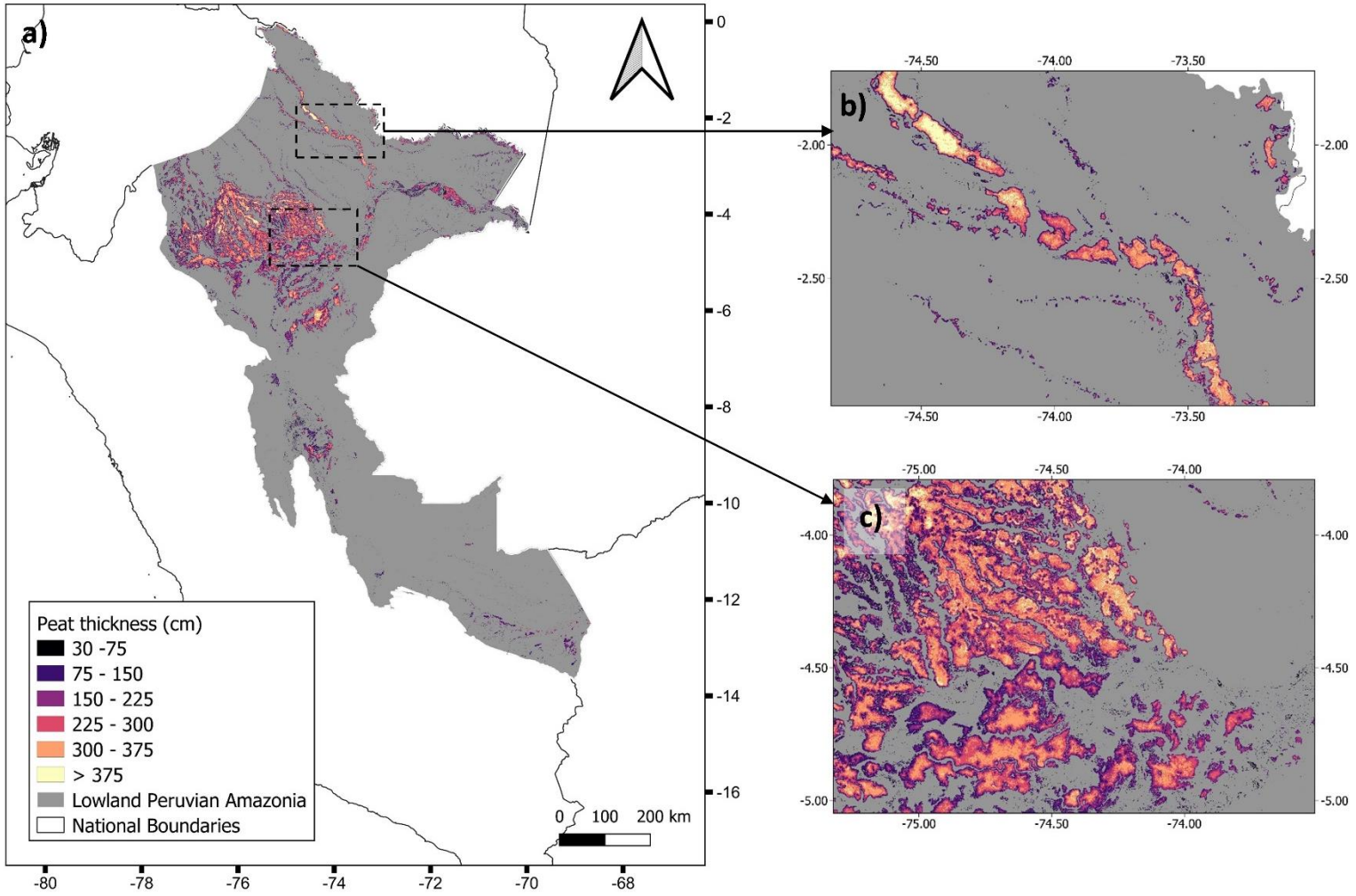

Figure 2: Distribution of peat thickness. a, predicted distribution of peat thickness across lowland Peruvian Amazonia estimated using random forest regression in Google Earth Engine (median of 1,000 k-folds). **b**, enlargement showing the Napo River. **c**, enlargement showing the Marañón and Tigre rivers. All maps were produced at a resolution of c. 100 m.

CO_2 emissions from land-use change are small but growing

Our analysis of land-use change data shows that a total peatland area of 1,052 km^2 was drained and/or cleared during 2000–2005, increasing to 1,667 km^2 by 2013–2016 (Table 1). Annual emissions from peat decomposition also increased from 3.26 million Mg CO_2 y^{-1} in 2000–2005 to 5.11 million Mg CO_2 y^{-1} in 2013–2016, while total estimated emissions accounted for 63.83 million Mg CO_2 during the period 2000–2016 mainly due to deforestation (Fig. 3b1, 3b2). Our analysis suggests rapid increases in CO_2 emissions from conversion to mining, urban areas and agriculture, increasing from 2000 to 2016 by 11 times (from 2,426 to 27,634 Mg CO_2 y^{-1}), 9 times (from 2,848 to 26,881 Mg CO_2 y^{-1}) and 5 times (from 77,807 to 411,528 Mg CO_2 y^{-1}), respectively (see Table S4 and S5 for further detail). These estimates exclude emissions from areas where natural peatland vegetation may have been misclassified in 2000 as secondary forest in the land cover dataset Geobosques (amounting to 1,353 km^2, Table S5). These misclassified areas were revealed by visual inspection of a Google map image of the department of Loreto by someone with local expert knowledge (Fig. 3a).

For those areas classified as forest in 2000, as accounted for in Peru's 2016 Forest Reference Emission Level report[29], emissions from peat decomposition represent 0.99–3.72% of total national CO_2 emissions from Lowland Peruvian Amazonian forests (i.e. from peat decomposition and biomass loss due to gross deforestation; Table 1).

Table 1: Mean CO_2 emissions from peat decomposition (95% CI) **and biomass loss across Lowland Peruvian Amazonia (LPA) for four periods between 2000 to 2016 following Geobosques dataset[30].** Peat emissions are from this study, biomass emissions are national estimates [a].

	Period			
	2000–2005	2005–2011	2011–2013	2013–2016
Duration (years)	5	6	2	3
Total peatland area with disturbance (km^2)	1,051.63	1,264.50	1,392.82	1,666.76
Total emissions from peat decomposition due to disturbance (x 10^6 Mg CO_2)	16.29 (6.94, 29.16)	23.27 (9.91, 41.61)	8.95 (3.73, 16.03)	15.33 (6.12, 27.59)
Peatland area with disturbance for categories classified as forest in 2000 (km^2)	158.46	404.38	536.48	808.92
Emissions from peat decomposition due to disturbance for categories classified as forest in 2000 (x 10^6 Mg CO_2)	1.25 (0.44, 2.25)	5.33 (1.94, 9.55)	2.98 (1.08, 5.35)	6.40 (2.21, 11.59)
Gross deforestation throughout LPA areas classified as forest in 2000 (km^2)[a]	2,483.38	3,945.33	1,915.72	3,303.01
Emissions from biomass loss due to gross deforestation throughout LPA (x 10^6 Mg CO_2)[b]	124.80	198.65	95.85	165.60
% due to peat decomposition for categories classified as forest in 2000	0.99 (0.35, 1.77)	2.61 (0.97, 4.59)	3.02 (1.12, 5.29)	3.72 (1.32, 6.54)

a 2016 Forest Reference Emission Level report of Peru[29].

b CO_2 emission from biomass includes both above- and below-ground biomass of living trees as calculated in the 2016 Forest Reference Emission Level report of Peru[29].

182

183

184

185

186

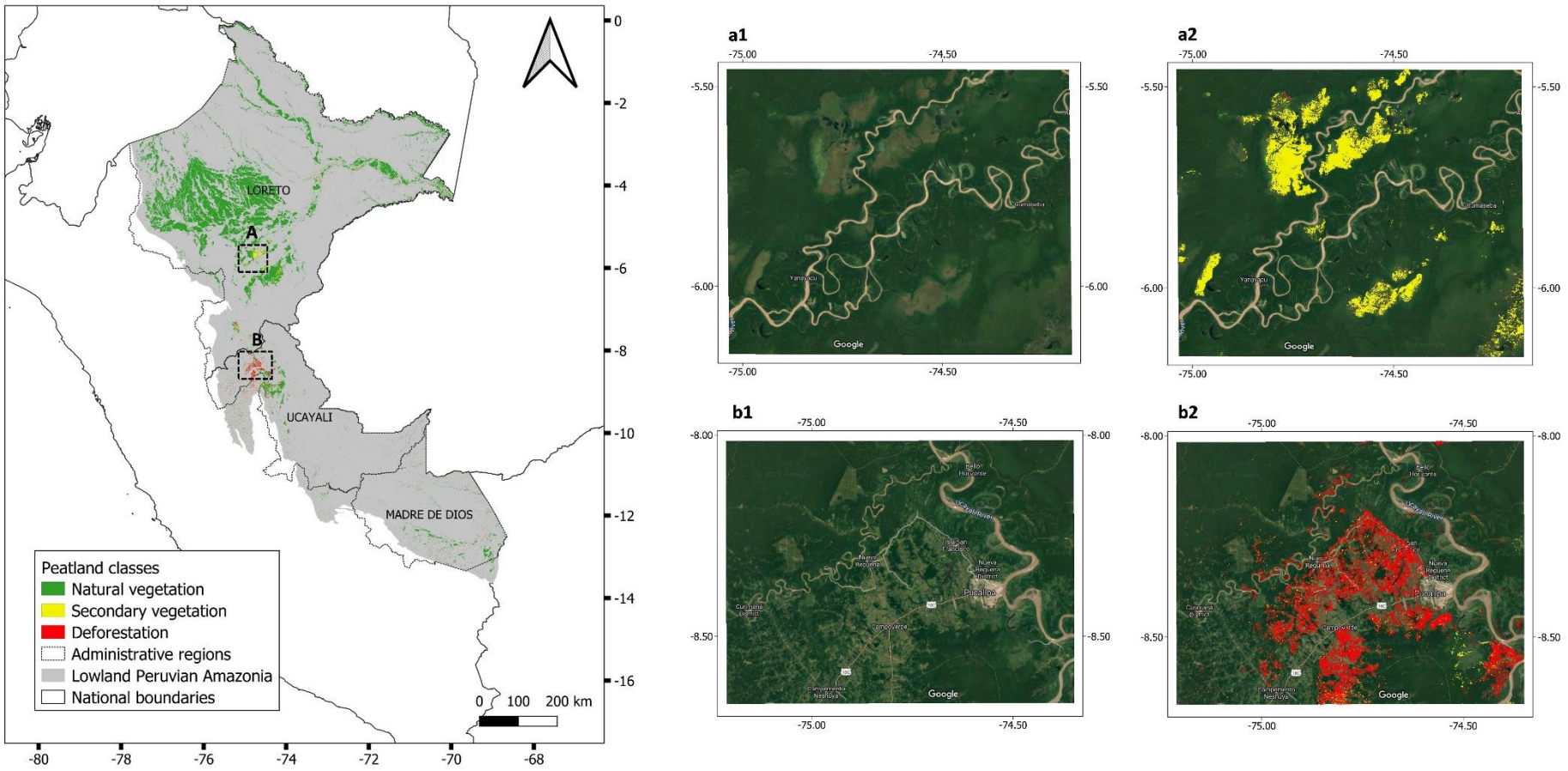

Figure 3: Distribution of peatlands classified as natural vegetation, secondary vegetation and deforestation based on the 2016 forest land and land use categories within Geobosques[30] in lowland Peruvian Amazonia. Non-peatland areas are shown in grey, and the relevant departments of Peru are labelled within the study area. Google map images show examples of (A) natural peatland vegetation misclassified as secondary forest (shown in a1, a2) around the Puinahua channel and the Ucayali river in the department of Loreto and (B) peatland areas correctly classified as deforestation (shown in b1, b2) near Pucallpa in the department of Ucayali.

193 ***Synthesis and future directions***

194

195 Our estimate of the total below-ground carbon stock of 5.38 (2.55–10.58) Pg C across the
196 LPA is 75% of a recent estimate of the entire above-ground C stock of Peru[31], and
197 approximately doubles previous estimates of the Peruvian tropical peat stock calculated for
198 the PMFB and the MDD regions only[2,19,22]. Our maps are driven by intensive field sampling
199 which has, for the first time, generated peat thickness data widely across LPA, and which
200 confirms that significant peatlands extend far beyond the relatively well-studied PMFB.
201 Across the main peat-forming landcover classes of pole forest, open peatland and palm
202 swamp, above-ground carbon densities (Table S2,[23]) are an order of magnitude lower than
203 respective peat carbon densities, totalling 0.45 Pg C (Table S2). Summing the above- and
204 below-ground carbon stocks gives a central estimate of 5.83 Pg C stored in LPA peatlands.

205 The quantitative uncertainties around the peatland carbon stock are reduced compared to
206 previous studies despite our study covering an area > 5 times greater [2,22]. Future
207 improvement may be gained by collecting field data where they are still lacking, notably the
208 northwest PMFB and parts of the Ucayali (e.g. around Pucallpa) and Morona basins. Unlike
209 previous studies[2,22] our study placed no constraints on which landcover classes peat can
210 form under, and we predict that around 2% of seasonally flooded forest is underlain by
211 peat. This suggests that the search for peat should not be solely limited to the well-known
212 peat-forming vegetation types of palm swamp, pole forest and open peatland. In addition to
213 landcover classification maps, we recommend that future fieldwork is informed by
214 examining maps and remote sensing imagery related to hydrology and inundation, such as
215 height above nearest drainage (HAND)[32], normalized difference water index (NDWI)[33] and
216 ALOS-PALSAR[34] (where possible multi-temporal images).

Our approach is driven by remote sensing layers with global coverage and can thus be readily adapted to other regions, provided sufficient field data are available for calibration and validation. Our results call for caution in treating all tropical peatlands as similar, and demonstrate the importance of field data. For example, distance to peatland edge has been found to correlate with peat thickness in other regions such as the Congo basin[3], and in most of the basins we studied in Peru. However, we found no significant linear relationship between peat thickness and distance to peatland edge for the data in the MDD basin (p > 0.1, R^2 = 0.005, Fig. S6c). Householder et al.[19] suggest that this may be because of specific geological conditions in this region: many of the deepest peats in the MDD are often located adjacent to upland (*terra firme*) terraces, close to the peatland edge. This means that the relationship between peat thickness and distance to peatland edge is more complex in MDD than in other regions. Past research points to geomorphological differences between northern and southern parts of Peruvian Amazonia[35]: while floodplains in northern Amazonia are often wide, rivers in southern Amazonia more often have narrow floodplains confined by terraces. We recommend that new transects should aim to target a range of landscape types (e.g. based on elevation maps) and where possible should cover the full cross-section of each individual peatland. In spite of this limitation, our random forest regression model for the MDD region performs reasonably well.

This study assesses CO_2 emissions resulting from peat decomposition due to land-cover change in Peru. Our results suggest that land cover change in the peatlands of the LPA has thus far been restricted to a few hotspot areas, with the largest area of deforestation identified near Pucallpa in the department of Ucayali, an area where recent ground observations confirm the presence of deforested peatlands ([26]; E. Honorio, pers. comm.). Access to these peatlands has been facilitated by the development of roads and the

241 increasing demand for land for commercial plantations (e.g. oil palm and rice[36,37],D. Garcia-
242 Soria, pers. comm.). Overall, the estimated emissions from peat decomposition remain low
243 in Peru but our analysis suggests that the annual emissions are increasing. These findings
244 have two implications for the conservation of these ecosystems. Firstly, the low current
245 emissions support the view that the extensive peatland complex of the LPA is an
246 emblematic example of hydrologically intact moist tropical forest with high structural
247 integrity and therefore should be a high conservation priority[23,38,39]. Investment is required
248 to promote protection and sustainable management of these widespread and extremely
249 carbon-dense ecosystems, before emissions rise over the coming decades[40,41]. Secondly, the
250 increasing threats and rising emissions from specific land-use transitions in some peatlands
251 mean that it is important to improve detection of deforestation and secondary vegetation
252 across the full range of peatland forest types, and to make more extensive measurements of
253 greenhouse gas emissions associated with specific land-use transitions across the different
254 forest types[7,8,9].

255 Taken together, our results indicate a carbon stock within the peatlands of LPA which is
256 three-quarters as large as the entire above-ground carbon stock of Peru[31] but contained
257 within just 5% of its land area. The peatlands also contribute substantial ecosystem and
258 floristic diversity to the Amazon[42,43]. While our study indicates that these peatlands remain
259 largely intact, they face varied and growing threats[15, 37]. Our mapping and carbon stock
260 estimates may be used to support the implementation and enforcement of recent
261 legislation aimed at reducing emissions[27] and should act to encourage national and
262 international investment in monitoring, protection and sustainable management of Peru's
263 peatlands, in order that they avoid a similar fate to the heavily degraded peatlands of
264 Southeast Asia[37].

Corresponding author

Correspondence to Adam Hastie.

Acknowledgments

This work was funded by NERC (Grant ref. NE/R000751/1)- ITL, AH, KHR, ETAM, CMA, TRB, GD, ECDG; Leverhulme Trust (Grant ref. RPG-2018-306)-KHR, LESC, CEW; Gordon and Betty Moore Foundation (Grant #5439, MonANPeru network)-TRB, ENHC, GF; Wildlife Conservation Society-ENHC; Concytec/British Council/Embajada Británica Lima/Newton Fund (Grant ref. 220-2018)-ENHC, JD; Concytec/NERC/Embajada Británica Lima/Newton Fund (Grant ref. 001-2019)-ENHC, ND; the governments of the United States of America (Grant No. MTO-069018) & Norway (Grant Agreement No. QZA-12/0882)-KH; and NERC Knowledge Exchange Fellowship (Grant Ref No. NE/V018760/1)-ENHC. We thank SERNANP, SERFOR and GERFOR for providing research permits, and the different indigenous and local communities, research stations and tourist companies for giving consent and allowing access to the forests. We acknowledge the invaluable support of technicians Julio Irarica, Julio Sanchez, Hugo Vásquez and Rider Flores, without whom much of the field work would not have been possible. We would like to thank the reviewers for the time and effort they took to carefully review the paper.

Author Contributions

A.H, I.T.L, E.N.H.C, E.T.A.M, K.H.R, T.R.B, L.E.S.C and C.E.W all contributed to the conception, development and design of the study. A.H and E.N.H.C performed the analysis with input

from E.T.A.M, K.H, I.T.L, L.E.S.C and P.R-V. A.H and E.N.H.C wrote the manuscript with input from all co-authors. New field data was collected by J.R, A.H, C.M.A, I.T.L, L.E.S.C, C.E.W, N.D, C.J.C-O, G.D, J.D.A, G.F, D.R, and J.G. E.H, O.L, F.D, J.P.J and M.T provided data.

Competing Interests

The authors declare no competing interests

References

1. Dommain, R., Couwenberg, J. & Joosten, H. Development and carbon sequestration of tropical peat domes in south-east Asia: links to post-glacial sea-level changes and Holocene climate variability. *Quat. Sci. Rev.* **30**, 999–1010 (2011).

2. Draper, F. C. *et al.* The distribution and amount of carbon in the largest peatland complex in Amazonia. *Environ. Res. Lett.* **9**, 124017 (2014).

3. Dargie, G. C. *et al.* Age, extent and carbon storage of the central Congo Basin peatland complex. *Nature* **542**, 86 (2017).

4. Ribeiro, K. *et al.* Tropical peatlands and their contribution to the global carbon cycle and climate change. *Glob. Chang. Biol.* **27**, 489–505 (2021).

5. Wang, S., Zhuang, Q., Lähteenoja, O., Draper, F. C. & Cadillo-Quiroz, H. Potential shift from a carbon sink to a source in Amazonian peatlands under a changing climate. *Proc. Natl. Acad. Sci.* **115**, 12407–12412 (2018).

6. IPCC. *2013 Supplement to the 2006 IPCC Guidelines for National Greenhouse Gas Inventories: Wetlands. Prepared by Hiraishi, T., Krug, T., Tanabe, K., Srivastava, N.,*

Baasansuren, J., Fukuda, M. and Troxler, T.G. (eds). (2014).

7. van Lent, J., Hergoualc'h, K., Verchot, L., Oenema, O. & van Groenigen, J. W. Greenhouse gas emissions along a peat swamp forest degradation gradient in the Peruvian Amazon: soil moisture and palm roots effects. *Mitig. Adapt. Strateg. Glob. Chang.* **24**, 625–643 (2019).

8. van Lent, J. Land-use change and greenhouse gas emissions in the tropics: Forest degradation on peat soils. PhD dissertation, Wageningen University. (2020).

9. Hergoualc'h, K. *et al.* Spatial and temporal variability of soil N2O and CH4 fluxes along a degradation gradient in a palm swamp peat forest in the Peruvian Amazon. *Glob. Chang. Biol.* **26**, 7198–7216 (2020).

10. Swails, E., Hergoualc'h, K., Verchot, L., Novita, N. & Lawrence, D. Spatio-Temporal Variability of Peat CH4 and N2O Fluxes and Their Contribution to Peat GHG Budgets in Indonesian Forests and Oil Palm Plantations. *Front. Environ. Sci.* **9**, 48 (2021).

11. Gaveau, D. L. A. *et al.* Major atmospheric emissions from peat fires in Southeast Asia during non-drought years: evidence from the 2013 Sumatran fires. *Sci. Rep.* **4**, 6112 (2014).

12. Page, S. E. *et al.* The amount of carbon released from peat and forest fires in Indonesia during 1997. *Nature* **420**, 61–65 (2002).

13. Mishra, S. *et al.* Degradation of Southeast Asian tropical peatlands and integrated strategies for their better management and restoration. *J. Appl. Ecol.* **58**, 1370–1387 (2021).

14. Dargie, G. C. *et al.* Congo Basin peatlands: threats and conservation priorities. *Mitig.*

330 *Adapt. Strateg. Glob. Chang.* **24**, 669–686 (2019).

331 15. Roucoux, K. H. *et al.* Threats to intact tropical peatlands and opportunities for their
332 conservation. *Conserv. Biol.* **31**, 1283–1292 (2017).

333 16. Griscom, B. W. *et al.* Natural climate solutions. *Proc. Natl. Acad. Sci.* **114**, 11645–
334 11650 (2017).

335 17. Girardin, C.A.J., Jenkins, S., Seddon, N., Allen, M., Lewis, S.L., Wheeler, C.E., Griscom,
336 B.W. & Malhi, Y. . Nature-based solutions can help cool the planet — if we act now.
337 *Nature* **593**, 191–194 (2021).

338 18. Murdiyarso, D., Lilleskov, E. & Kolka, R. Tropical peatlands under siege: the need for
339 evidence-based policies and strategies. *Mitig. Adapt. Strateg. Glob. Chang.* **24**, 493–
340 505 (2019).

341 19. Householder, J. E., Janovec, J. P., Tobler, M. W., Page, S. & Lähteenoja, O. Peatlands
342 of the Madre de Dios River of Peru: Distribution, Geomorphology, and Habitat
343 Diversity. *Wetlands* **32**, 359–368 (2012).

344 20. Hess, L. L. *et al.* Wetlands of the Lowland Amazon Basin: Extent, Vegetative Cover,
345 and Dual-season Inundated Area as Mapped with JERS-1 Synthetic Aperture Radar.
346 *Wetlands* **35**, 745–756 (2015).

347 21. Gumbricht, T. *et al.* An expert system model for mapping tropical wetlands and
348 peatlands reveals South America as the largest contributor. *Glob. Chang. Biol.* **23**,
349 3581–3599 (2017).

350 22. Lähteenoja, O. *et al.* The large Amazonian peatland carbon sink in the subsiding
351 Pastaza-Marañón foreland basin, Peru. *Glob. Chang. Biol.* **18**, 164–178 (2012).

23. Coronado, E. N. H. *et al.* Intensive field sampling increases the known extent of carbon-rich Amazonian peatland pole forests. *Environ. Res. Lett.* **16**, 74048 (2021).

24. Hergoualc'h, K., Gutiérrez-Vélez, V. H., Menton, M. & Verchot, L. V. Characterizing degradation of palm swamp peatlands from space and on the ground: An exploratory study in the Peruvian Amazon. *For. Ecol. Manage.* **393**, 63–73 (2017).

25. Baker, T.R., del Castillo Torres, D., Honorio Coronado, E., Lawson, I., Brañas, M.M., Montoya, M., Roucoux, K. The challenges for achieving conservation and sustainable development within the wetlands of the Pastaza Marañón basin, Peru. pp. 155-175 *in 'Peru: Deforestation in times of climate change' (ed. A. Chirif), International Work Group for Indigenous Affairs,*. (2019).

26. López Gonzales, M.; Hergoualc'h, K.; Angulo Núñez, Ó.; Baker, T.; Chimner, R.; del Águila Pasquel, J.; del Castillo Torres, D.; Freitas Alvarado, L.; Fuentealba Durand, B.; García Gonzales, E.; Honorio Coronado, E.; Kazuyo, H.; Lilleskov, E.; Málaga Durán, F. What do we know about Peruvian peatlands? Bogor, Indonesia. Retrieved from https://www.cifor.org/publications/pdf_files/OccPapers/OP-210.pdf (2020).

27. MINAM. Decreto Supremo N° 006-2021-MINAM (2021).

28. Lähteenoja, O., Ruokolainen, K., Schulman, L. & Oinonen, M. Amazonian peatlands: an ignored C sink and potential source. *Glob. Chang. Biol.* **15**, 2311–2320 (2009).

29. MINAM. Peru's submission of a Forest Reference Emission Level (FREL) for reducing emissions from deforestation in the Peruvian Amazon. 77 pages (2016).

30. MINAM. *Coberturas de uso y cambio de uso de la tierra para los periodos 2000-2005, 2005-2011, 2011-2013, 2013-2016. Monitoreo de los cambios sobre la cobertura de*

los bosques peruanos – Geobosques. (2020).

31. Csillik, O., Kumar, P., Mascaro, J., O'Shea, T. & Asner, G. P. Monitoring tropical forest carbon stocks and emissions using Planet satellite data. *Sci. Rep.* **9**, 17831 (2019).

32. Donchyts, Gennadii., Winsemius, Hessel., Schellekens, Jaap., Erickson, Tyler., Gao, Hongkai., Savenije, Hubert., and van de Giesen, N. 'Global 30m Height Above the Nearest Drainage (HAND)'. in (Geophysical Research Abstracts, Vol. 18, EGU2016-17445-3, 2016, EGU General Assembly, 2016).

33. Drusch, M. *et al.* Sentinel-2: ESA's Optical High-Resolution Mission for GMES Operational Services. *Remote Sens. Environ.* **120**, 25–36 (2012).

34. Shimada, M. *et al.* New global forest/non-forest maps from ALOS PALSAR data (2007–2010). *Remote Sens. Environ.* **155**, 13–31 (2014).

35. Toivonen, T., Mäki, S. & Kalliola, R. The riverscape of Western Amazonia – a quantitative approach to the fluvial biogeography of the region. *J. Biogeogr.* **34**, 1374–1387 (2007).

36. Vijay, V., Reid, C. D., Finer, M., Jenkins, C. N. & Pimm, S. L. Deforestation risks posed by oil palm expansion in the Peruvian Amazon. *Environ. Res. Lett.* **13**, 114010 (2018).

37. Lilleskov, E. *et al.* Is Indonesian peatland loss a cautionary tale for Peru? A two-country comparison of the magnitude and causes of tropical peatland degradation. *Mitig. Adapt. Strateg. Glob. Chang.* **24**, 591–623 (2019).

38. Watson, J. E. M. *et al.* The exceptional value of intact forest ecosystems. *Nat. Ecol. Evol.* **2**, 599–610 (2018).

39. Hansen, A. J. *et al.* A policy-driven framework for conserving the best of Earth's remaining moist tropical forests. *Nat. Ecol. Evol.* **4**, 1377–1384 (2020).

40. Maxwell, S. L. *et al.* Degradation and forgone removals increase the carbon impact of intact forest loss by 626%. *Sci. Adv.* **5**, 10 (2019).

41. Grantham, H. S. *et al.* Anthropogenic modification of forests means only 40% of remaining forests have high ecosystem integrity. *Nat. Commun.* **11**, 5978 (2020).

42. Lähteenoja, O. & Page, S. High diversity of tropical peatland ecosystem types in the Pastaza-Marañón basin, Peruvian Amazonia. *J. Geophys. Res. Biogeosciences* **116**, (2011).

43. Draper, F. C. *et al.* Peatland forests are the least diverse tree communities documented in Amazonia, but contribute to high regional beta-diversity. *Ecography,* **41**, 1256–1269 (2018).

Methods

Fieldwork

Between 2019 and 2021, we collected 445 new ground reference points (GRPs) within LPA (Fig. 1, 294 of which were presented by ref.[23]) collecting data on the substrate (i.e peat thickness, where peat is present) and vegetation type (e.g. palm swamp). We focused data collection on regions with no existing GRPs, where peat was believed to be present based on remote sensing imagery (e.g. various Landsat 8 [Fig. S7] and Sentinel 2 bands), including

416 the Napo, Putumayo, Tapiche and Tigre river basins (Fig. 1, Fig. S1), using the only available
417 means of access, i.e. via rivers and streams. We also collected new data on peat thickness
418 and carbon concentration from under-sampled peatland ecosystems (e.g. peatland pole
419 forest). We made the sampling as spatially representative as possible within the constraints
420 of logistical feasibility, personal safety and accessibility, which are substantial in these
421 remote regions of Peru. The previously published datasets which we incorporated here
422 were also subject to the same constraints.

423 Where present, peat thickness was measured with an auger or Russian-type peat corer,
424 either along transects perpendicular to the river at intervals of 200–500 m, or at the four
425 corners and centre of the vegetation plots (see below) in which case the value for peat
426 thickness used is the mean of five point measurements. Working along transects leading
427 away from the river and into the peatlands allowed us to sample across wide hydrological
428 and topographic gradients, including both minerotrophic and ombrotrophic ecosystems. At
429 91 of these GRPs, we conducted 1 ha, 0.5 ha or 0.1 ha vegetation plot surveys (collecting
430 floristic data) for quantitative classification of ecosystem type[23,43]. Additionally, we used 218
431 previously published GRPs[2,22,28] (24 with floristic data) collected using a similar transect-
432 based sampling strategy in northern Peru and 465 GRPs[19] (148 with floristic data) collected
433 in southern Peru, amounting to a total of 1,128 GRPs (Fig. 1). Of these, 887 GRPS (Fig. S8)
434 indicated the presence of peat (defined as an organic layer ≥ 30 cm thick[44]). Two examples
435 of peat thickness measurement transects in the Napo basin are shown in Figure S7.

436 The majority of peat thickness observations do not have corresponding carbon
437 concentration measurements and thus we cannot enforce a precise cut-off in terms of
438 carbon content. However, we visually identified peat and underlying sediments in the field

on the basis of their physical properties (e.g. colour, structure, texture) and composition (e.g. wood, roots, mineral components)[45,46]. At 35 vegetation plots identified by fieldworkers as being on peat, we took sediment samples in the near-basal peat, transition zone and underlying mineral sediment (typically silts or clays) and measured loss on ignition (LOI) in each to test the visual assessments. The peat, transition zone and mineral samples had mean LOI values of 70%, 28% and 13% respectively (see Table S6). This gives us confidence that fieldworkers in this region are able to visually identify peat (in this case, soil with an LOI of at least 50%), as there is typically a clear and distinct transition to mineral sediment in Peruvian peatlands.

Map of predicted peatland extent in lowland Peruvian Amazonia

We created a 50 m resolution map (Fig. S2) of predicted peatland extent in LPA (defined here as the area covered by two of the ecozones recognized by Peru's Ministry of Environment: Ecozone Selva Baja and Ecozone Hidromórfica[47]). Firstly, we ran a supervised random forest (RF) algorithm (200 trees) in Google Earth Engine to predict the distribution of five classes: peat below forest (PBF), peat below non-forest (i.e. herbaceous vegetation and shrubland, PBNF), non-peat below forest (NBF), non-peat below non-forest (NBN) and open water (WA). The model was trained and validated (50/50 split of polygons) using peat thickness measurements and information on the overlying vegetation, and driven using a stack of seven remote sensing layers including two Sentinel-2 indices (NDVI & NDWI[33]), three ALOS PALSAR-2 bands (HH, HV, HH/HV[34]), SRTM 30 m digital elevation[48] (Table S7), and an extended version of a landcover classification produced previously[23] (Fig. S9; Supplementary Information has further details). The PBF and PBNF categories were amalgamated to form the map of total peatland extent in Fig. S2. We calculated 5th and 95th

462 confidence interval percentiles for peatland area using the area and accuracy of each class,
463 applying the method described in ref. [49] (equations 9–13), following ref. [2] and
464 recommended by the Global Forest Observations Initiative.

465 ***Model of peat thickness distribution***

466 Testing showed that peat thickness increases with distance to peatland edge (R^2 = 0.13, p <
467 0.0001, Fig. S6), indicating that the deepest peat is typically found in the centre of a
468 peatland. We thus calculated distance to peatland edge for each model grid, using our map
469 of peatland extent. We used the 1,128 peat thickness measurements as training data,
470 supplemented with points that we assumed to lack peat located along known rivers and
471 urban areas (based on a combination of local knowledge and inspection of Sentinel-2 and
472 Landsat 8 images), amounting to a final dataset of 1,359 points. The model was run at 100 m
473 resolution in Google Earth Engine and driven by the stack of remote sensing layers, with two
474 additional layers: distance to peatland edge, and height above nearest drainage (HAND[32])
475 (Table S8).

476 In order to robustly test model performance, we performed a series of validations which
477 accounted for spatial autocorrelation. Training the model using data only from within the
478 PMFB (n = 717) and testing against data from outside the PMFB in Northern Peru (Napo,
479 Putumayo and upper Amazon basins, n = 155), the model performed relatively well
480 (Observed *vs* Predicted peat thickness, p < 0.0001; R^2 = 0.56, Fig. S10a). However, the same
481 model (trained using only PMFB data) was unable to predict variation in peat thickness
482 observed in the Madre De Dios (MDD) basin data (n = 478, p > 0.50; R^2 = 0.00, Fig. S10b). For
483 this reason, we decided to run two separate models for the final analysis, one using data
484 only within the MDD basin (n = 477, no. model trees = 100), and another using all other data

points (n = 867, no. model trees =50). Model performance was lower in the model which used only MDD data ($p < 0.0001$; $R^2 = 0.38$, RMSE = 70%, Fig. S5b) than that using all other data points (Observed Vs Predicted peat thickness, $p < 0.0001$; $R^2 = 0.66$, RMSE = 66%, Fig. S5a). We independently validated both models by training each with 80% of the data (randomly selected) and testing with the remaining 20% (Fig. S5c, d).

To account for the uncertainty associated with our estimate of peat thickness distribution, we ran a k-fold analysis as in[50], splitting the data into 1,000 folds, and therefore generating 1,000 predictions of peat thickness per pixel. We took the median, 5th and 95th percentiles of the 1,000 predictions to represent our best estimate (Fig. 2a), minimum (Fig. S3a) and maximum (Fig. S3b) peat thickness distributions. We subsequently masked the maps of peat thickness distribution using the map of peatland extent (Fig. S2), thus restricting our model to only regions predicted to contain peat.

Below-ground carbon stock

A dataset of 68 stratigraphic profiles of carbon concentration (%) and dry bulk density (DBD, g cm^{-3}) was compiled using data from refs [2,22,23,28,51] (see Table S9). This includes ten new peat profiles collected as part of this study and described in[23] (see Table S4 of Honorio Coronado et al., 2021[23]). We calculated peat carbon stock (PC, Mg C ha^{-1}) from the peat cores by multiplying peat thickness (cm) by DBD and carbon concentration evaluated at regular intervals down the peat profile to the base of the peat. Laboratory conditions varied depending on the study and can be found in the original papers, along with information on protocols. The studies used a variety of standard methodologies to determine sample carbon concentrations. In line with our definition of peat, we only retained cores in which

507 the peat was ≥ 30 cm thick, with a mean LOI of ≥ 50%, and those collected using a Russian
508 corer to ensure that DBD measurements were based on a reliable volumetric sample.

509 We performed a sensitivity analysis to test which of the three components of PC (i.e. peat
510 thickness, DBD and carbon concentration) was most important. Peat thickness was found to
511 be the most important determinant of total PC ($p < 0.0001$; $R^2 = 0.81$, Fig. S11). We thus
512 used our model of peat thickness distribution to estimate total PC for each 100 m grid-cell
513 and then summed across the entire LPA to produce a total value for the peat carbon stock.

514 In order to produce uncertainty bounds for our estimate of the total peat C stock, we ran a
515 Monte Carlo analysis which accounted for the uncertainty in each stage of our
516 methodology. We ran 1,000 simulations for PC, constrained using the standard error of the
517 b-estimates from the regression equation (peat thickness *vs* PC, Fig. S11). This was
518 performed twice, once using the 5th and then the 95th percentile distribution of peat
519 thickness calculated previously (Fig. S3). These 1,000 PC simulations were in turn multiplied
520 by 1,000 simulations of peatland area per grid, constrained by the confidence intervals
521 calculated previously. Finally, the maps of the 5th and 95th percentile of peat C stock per grid
522 were summed across LPA to derive the final minimum and maximum uncertainty bounds.

523

524 ***Activity data and emissions from peat decomposition***

525 To estimate changes in forest cover, we used reports of activity data provided by Peru's
526 national monitoring platform, Geobosques[30]. These reports were generated using Landsat 7
527 and 8 images from 2001 to 2016 at 30 m resolution, with cumulative areas of different land
528 uses for the year 2000[30]. In these data, Peruvian Amazonia is classified into 11 land uses for
529 the periods 2000–2005, 2005–2011, 2011–2013, and 2013–2016. Figure 3 shows our

predicted peatland map (produced by re-running our model at 30 m resolution to match the activity dataset) grouping the categories that represent natural vegetation (forest, forest on wetland, wet savannah, water body, non-forest on wetland), secondary vegetation, and deforested areas (agriculture, pasture, urban areas, mining areas, bare ground).

Emission factors for organic soils were taken from Chapter 2 of the 2013 Supplement to the 2006 IPCC Guidelines for the National GHG Inventory for Wetlands[6]. The values range from 7.5 Mg C ha^{-1} y^{-1} for secondary vegetation to 9.6 Mg C ha^{-1} y^{-1} for deforested peatlands (Table S4). These IPCC values are intended to be used for drained peatlands, but peatland disturbance in Peru does not necessarily entail drainage. Nonetheless, undrained secondary forests on peat in Indonesia lose soil carbon (1.4 Mg C ha^{-1} y^{-1}; [10]) at a similar rate to shallow-drained plantations (1.5 Mg C ha^{-1} y^{-1}; [6]), and CO_2 emissions in highly degraded undrained peatlands in Peru (e.g. degraded *Mauritia*-dominated palm swamps classified as secondary vegetation: 7.1 Mg C ha^{-1} y^{-1}; [8]) fall within the range of the values of deforested drained peatlands in Indonesia (1.5–14.0 Mg C ha^{-1} y^{-1}; [6], Table S5). Therefore, we assume the IPCC emission factors are acceptable estimates for drained or undrained peatlands in Peru, which is reasonable given that it matches the available evidence.

Total CO_2 emissions following land use change due to inferred peat decomposition were estimated following the equation 2.3 from Chapter 2 in the IPCC Wetlands Supplement[6]:

$$PDE = \sum_{ij=0}^{n} A_{ij} * EF_{ij} * t * 44/12 \quad (1)$$

Where *PDE* is total CO_2 emissions from peat decomposition (Mg CO_2); *A* is the area (ha) on peatlands of the original land-use category-*i* that was converted into category-*j* during the time period *t* (years); *EF* is the mean annual emission factor of peat decomposition assigned to the conversion from category-*i* to category-*j* (Mg C ha^{-1} y^{-1}) and converted to CO_2 by multiplying by the atomic mass factor of 44/12 [52,53]. For example, within peatlands (according to our map), forest on wetland (ecosystem saturated with water and assumed zero CO_2 emissions) that is converted to mining area (ecosystem assumed similar to drained grasslands with emissions of 9.6 Mg C ha^{-1} y^{-1}) will receive an *EF* value of 4.8 Mg C ha^{-1} y^{-1} following [52] (Table S5).

Data availability

An interactive map of modelled peatland extent (50 m resolution) can be viewed here: https://code.earthengine.google.com/a07b25e62adbe714afa77e4a3e423b1b and source map downloaded here:

An interactive map of modelled landcover class (50 m resolution) can be viewed here: https://code.earthengine.google.com/f3a655bbf36db6121be1d7fd09991530 and source map downloaded here: https://datashare.ed.ac.uk/handle/10283/4364

An interactive map of modelled peat thickness distribution (100 m resolution) can be viewed here: https://code.earthengine.google.com/8845760a7e086df8b1e66075985ea705 and source maps downloaded here: https://datashare.ed.ac.uk/handle/10283/4364

An interactive map of modelled peat carbon (100 m resolution) can be viewed here: https://code.earthengine.google.com/394ed8b119c1913f7c5f5b6a969ec19f and source maps downloaded here: https://datashare.ed.ac.uk/handle/10283/4364

The MINAM Geobosques[30] raster file can be downloaded here: https://geobosques.minam.gob.pe/geobosque/view/descargas.php?122345gxxe345w34gg

Code availability

The above Google Earth Engine links include code for some basic analysis of the maps. Code for other parts of the analysis will be made available upon reasonable request to the corresponding author.

Additional references for methods

44. Page, S. E., Rieley, J. O. & Banks, C. J. Global and regional importance of the tropical peatland carbon pool. *Glob. Chang. Biol.* **17**, 798–818 (2011).

45. Troels-Smith, J. Characterisation of unconsolidated sediments. *Danmarks Geol. Undersogelse* **IV**, 73 (1955).

46. Kershaw., A. . A modification of the Troels-Smith system of sediment description and portrayal. *Quat. Australas.* **15**, 63–68 (1997).

47. Málaga, N., Giudice, R., Vargas, C., y Rojas, E. *Estimación de los contenidos de carbono de la biomasa aérea en los bosques de Perú. Lima: Ministerio del Ambiente del Perú.* (2014).

48. Farr, T. G. *et al.* The Shuttle Radar Topography Mission. *Rev. Geophys.* **45**, (2007).

49. Olofsson, P., Foody, G. M., Stehman, S. V & Woodcock, C. E. Making better use of accuracy data in land change studies: Estimating accuracy and area and quantifying uncertainty using stratified estimation. *Remote Sens. Environ.* **129**, 122–131 (2013).

50. Rodríguez-Veiga, P. *et al.* Carbon Stocks and Fluxes in Kenyan Forests and Wooded Grasslands Derived from Earth Observation and Model-Data Fusion. *Remote Sensing* vol. 12 (2020).

51. Bhomia, R. K. *et al.* Impacts of Mauritia flexuosa degradation on the carbon stocks of

freshwater peatlands in the Pastaza-Marañón river basin of the Peruvian Amazon. *Mitig. Adapt. Strateg. Glob. Chang.* **24**, 645–668 (2019).

52. Ministry of Environment and Forestry. Indonesia. *MoEF, 2016, National Forest Reference Emission Level for Deforestation and Forest Degradation: In the Context of Decision 1/CP.16 para 70 UNFCCC (Encourages developing country Parties to contribute to mitigation actions in the forest sector), Directorate* . (2016).

53. IPCC. *IPCC guidelines for National Greenhouse Gas Inventories. Agriculture, forestry and other land use (AFOLU), Vol. 4, Eggleston, S., L. Buendia, K. Miwa, T. Ngara, and K. Tanabe (eds.). Prepared by the National Greenhouse Gas Inventories Programme, Institu*. https://www.ipcc-nggip.iges.or.jp/public/2006gl/vol4 (2006).